JOURNAL OF SOLID STATE CHEMISTRY **126,** 33–37 (1996)
ARTICLE NO. 0306

3D Data Set of Diffuse X-Ray Scattering of Calcium-Stabilized Zirconia

Th. Proffen, R. B. Neder, and F. Frey

Institut für Kristallographie und Mineralogie, LMU München, Theresienstraße 41, D-80333 München, Germany

Received September 5, 1995; in revised form May 28, 1996; accepted June 3, 1996

Measurements of a 3-dimensional data set of disorder diffuse scattering of stabilized zirconia doped with 15 mol% CaO were carried out on a CAD4 diffractometer using a 2-dimensional position-sensitive detector (PSD). Calculations presented in this paper indicate that all observed diffuse data can be explained by the superposition of diffuse maxima located in symmetrically equivalent [1$\bar{1}$0] zones corresponding to satellite vectors of ±(0.4 0.4 ±0.8). The halfwidth of the diffuse maxima perpendicular to the layers of the [1$\bar{1}$0] zone is in the same range as within the layers.

INTRODUCTION

The cubic phase of pure ZrO_2 is thermodynamically stable only at temperatures above 2643 K but can be retained to room temperature by doping with various oxides of di- and trivalent metals (e.g., Ca, Mg, Y). The average structure is of the flourite-type structure, space group $Fm\bar{3}m$, with metal atoms on (0, 0, 0) and oxygens on $(\frac{1}{4}, \frac{1}{4}, \frac{1}{4})$. The stabilization is due to oxygen vacancies introduced by the dopant metal ion which occupies a zirconium site (1). The zirconium ions are located on seven-coordinated cation sites in the locally distored fluorite-type structure (2).

In previous studies (3–5) we analyzed the diffuse scattering of calcium-stabilized zirconia by a model of a distribution of correlated microdomains based on single- and double-oxygen vacancies within the cubic matrix of the crystal. The observed diffuse scattering can be divided in two parts: broad diffuse bands and diffuse maxima which can be indexed as satellites with vectors ±(0.4 0.4 ±0.8). These diffuse peaks are generally assumed to be maximal within the measured layers of the [1$\bar{1}$0] zone which was verified for two diffuse maxima of the 0th layer in previous neutron scattering experiments (3). Other authors (6, 7), however, report more extended diffuse features of zirconia and conclude that the observed diffuse maxima within the layers of the [1$\bar{1}$0] zone are merely sections of these extended diffuse scattering. The data for the yttrium stabilized zirconia (6, 7) show broad diffuse scattering while the data for calcium stabilized zirconia (7) show much more sharply peaked maxima. The dark lines visible for YSZ are hardly visible for CSZ. The relative intensity of corresponding diffuse scattering changes from YSZ to CSZ. Note that the composition of the CSZ in (7) is different from the samples reported here. The absence of "real" diffuse maxima which are not created by intersections of extended diffuse scattering, however, would shed a new light on the defect model and, furthermore, all our earlier quantitative analyses of the diffuse scattering of zirconia would have to be reconsidered. In order to answer this question and to get a more reliable insight into the defect structure of stabilized zirconia, a 3-dimensional data set of the diffuse scattering of calcium-stabilized zirconia was collected at a CAD4 diffractometer using an area detector.

EXPERIMENTAL AND MEASUREMENTS

The zirconia samples with a composition of $Zr_{0.85}Ca_{0.15}O_{1.85}$, grown by the skull melting method, were delivered by Djevahirdjan S. A., Monthey, Switzerland. The size of the used crystal was about 200 × 100 × 100 μm^3. The diffraction experiments were carried out at a CAD4 diffractometer using a graphite monochromator and Mo$K\alpha$ radiation (0.7093 Å). The data collection was done with an area detector system which consists of a 2-dimensional proportional chamber manufactured by Bio-Logic, Claix, France. The readout electronics and a PC-based data acquisition unit was delivered by FAST-Com Tech. The detector was mounted at $2\Theta = 30°$ at a distance of 320 mm from the sample. For the combined control of the diffractometer and the detector system we used the DIFFUSE-routines (8) which are extensions to the CAD4 control program (EXPRESS 5.1). These routines enable the user to set any zone axis perpendicular to the scattering plane. Measurements can be performed by the oscillation method with the chosen zone axis as oscillation axis. In the present study the [1$\bar{1}$0] zone was aligned parallel to ω axis. A data collection was carried out for a 90° sector at 87 evenly spaced ω positions. At each ω

0022-4596/96 $18.00

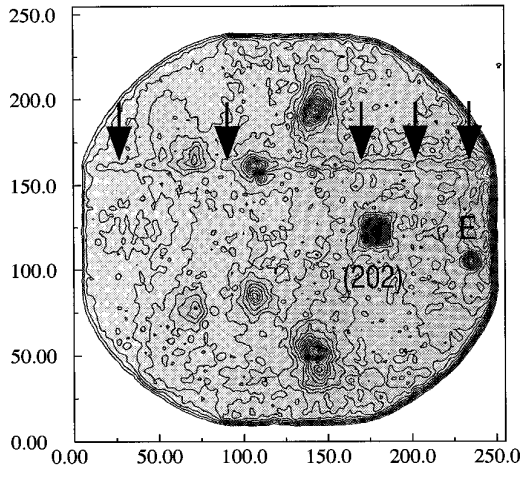

FIG. 1. Single area detector measurement of zirconia at a fixed ω position; measuring time was 1 h. The intensities are given in steps of 50 counts; the lowest intensity level corresponds to 5 counts. For additional information see the text.

position the detector was exposed for 60 min with the crystal at rest. The raw data from the detector for a single ω position are shown in Fig. 1. The (202) Bragg reflection and diffuse scattering can be observed. Beside these parts of intensity coming from the sample, two other features can be seen in Fig. 1: The first is a line of slightly higher intensity marked by several black arrows corresponding to a wire inside the detector with a different mechanical tension. The second feature is a spot of lower intensity marked with "E" due to electronic problems. The extraction procedure for a certain reciprocal plane is described in the following section.

DATA EVALUATION AND RESULTS

For the data evaluation of measurements of diffuse scattering with the 2-dimensional detector, the program MPAUS (9) was developed. This program has several features: it allows one to refine the detector parameters (i.e., sample–detector distance, resolution) and all conversions between detector coordinates and coordinates in reciprocal space, and it allows one to extract the intensities from any reciprocal plane out of the set of measured data. Details about the program can be found in (9). Here we want to focus on the extraction of reciprocal planes. The reported measurement consists of 87 single "images" of the detector taken at different ω angles with $[1\bar{1}0]$ as the zone axis. The program runs through all pixels of the detector and calculates the reciprocal coordinates. A point is considered to be within the extracted plane if it matches the inequality

$$|(hkl)[uvw] - S| < \varepsilon. \qquad [1]$$

(hkl) is the reciprocal point to be tested, $[uvw]$ the zone axis, S the layer which should be extracted, and ε a parameter which determines how "exact" the point has to be within the extracted plane. For a fixed ω value, the (hkl) from a single detector image that fulfill Eq. [1] form an arc within the plane normal to the $[uvw]$ direction. All data points from several ω positions are mapped onto a suitable grid in the reciprocal layer to be extracted. All (hkl) with identical projection along $[uvw]$, i.e., projection onto $\varepsilon = 0$, are averaged. The value ε gives the thickness of the slab that is averaged. A suitable value for ε depends on the resolution of the detector. If ε is too small, a few of the pixels on the finite detector grid will fulfill Eq. [1], resulting in apparently unobserved spots on the extracted plane. In this study this value was $\varepsilon = 0.05$, determined by several calculations with different ε values. The results for the 0th up to the 2nd layer of the $[1\bar{1}0]$ zone in steps of 0.2 are shown in Fig. 2. In the 0th and 2nd layer strong Bragg reflections are visible beside diffuse maxima which are comparable to the maxima measured with a single counter in our previous study (5), but there is also strong diffuse scattering in between. As described in the previous section some instrumental effects are visible (i.e., the radial streaks and small minima) due to the nonoptimum detector or electronic problems. The diffuse scattering, however, can clearly be separated. The diffuse maxima are visible throughout several of the reciprocal layers with two distinct variations. First, note the behavior of the diffuse maximum at 1.4 1.4 2.2, the strongest diffuse maximum in the zero layer (Fig. 2). The intensity drops continuously up to the 0.4 layer. A change of position is not observed. This clearly shows that this feature is a maximum with approximately equal FWHM in all directions and not a cross section of an extended diffuse feature. Second, note the pair of diffuse maxima at 1.4 1.4 1.8 and at 1.6 1.6 1.2. The intensity of the maximum at 1.4 1.4 1.8 is 134, 139, and 125 counts in the layers 0, 0.2, and 0.4, respectively. The corresponding intensities for the maximum at 1.6 1.6 1.2 and on the midpoint between these two maxima are 125, 131, 122 and 103, 107, 135. The intensities of the two maxima drop without change of position from the zero layer to the layer 0.4. At the layer 0.4 a broad maximum at the position between these two maxima is observed. Due to the broad FWHM of the maxima, the overlap of the three maxima in the layer 0.2 causes a slight increase of the intensity of the maxima at 1.4 1.4 1.8 and at 1.6 1.6 1.2. Note that the increase, however, is within the errors of counting statistics. We interpret this behavior as overlapping maxima from other symmetrically equivalent $[1\bar{1}0]$ zone axes. Since the maxima are broad, the overlap of the three maxima gives the appearance of a continuous intensity distribution around $\frac{3}{2}(111)^*$.

As mentioned, a main goal was to distinguish whether the observed additional diffuse scattering between the 0th

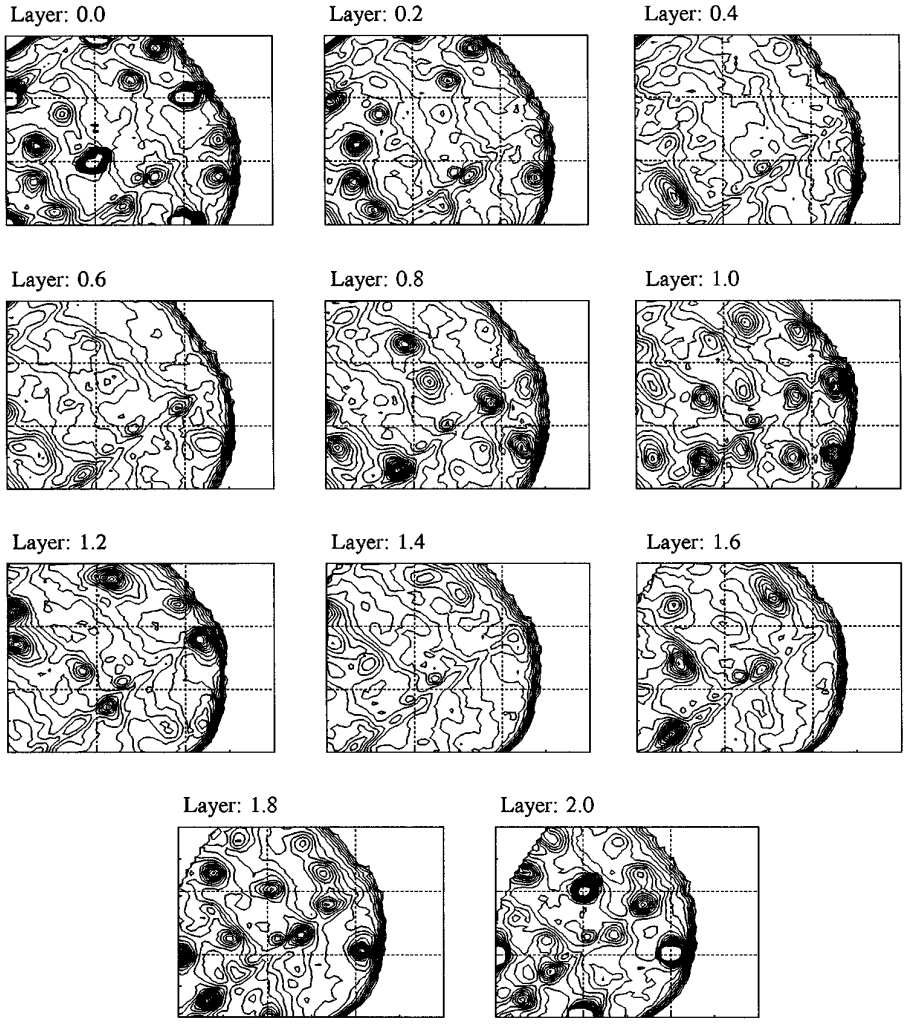

FIG. 2. Extracted 0th to 2nd layer of the [$1\bar{1}0$] zone of zirconia. The intensities are given in steps of 5 counts; the lowest intensity level corresponds to 20 counts. For each of the layers the following notations hold: The horizontal axis is parallel to [110], the vertical parallel to [001]. The lower left corner corresponds to the intersection with a line parallel to the [$1\bar{1}0$] axis through the 111 reflection. The broken lines mark intervals of one reciprocal lattice unit. Thus, in the layer 0.0 the corners of the plot are: lower left 111, lower right 441, upper left 114, upper right 444. In the layer 2.0 the corresponding corners are: 201, 531, 204, and 534.

and 2nd layer of the [$1\bar{1}0$] zone is caused by diffuse maxima of symmetrically equivalent [110] zones or is due to a new kind of defect structure. We tested the former hypothesis by calculating the intersection of the measured layers with all diffuse maxima that correspond to symmetrically equivalent [$1\bar{1}0$] zones. The following restrictions apply: All diffuse maxima were assumed to be isotropic Gaussians $G(h, k, l)$ with a halfwidth of 0.25 reciprocal lattice units and the intensity of the diffuse maxima were taken from our previous measurements (5). The results of these calculations (Fig. 3) show qualitatively that the observed strong diffuse maxima can be explained by the full set of symmetrically equivalent diffuse maxima. Specifically note that the intensity distribution around $\frac{3}{2}(111)^*$ is reproduced quite well, explaining the apparently ring-type diffuse intensity distribution by an overlap of different diffuse maxima. A further important observation is that the set of all symmetrically equivalent diffuse maxima does not create any additional unobserved diffuse features. The intensity of the diffuse maxima, however, is not always reproduced accurately due to the simplified model, i.e., calculation with symmetric Gaussians, no background correction, and no correction for the detector effects mentioned in the last section.

DISCUSSION

The results of this study clearly indicate that the diffuse maxima indexed by satellite vectors $\pm(0.4\ 0.4\ \pm 0.8)$, as observed for calcium-stabilized zirconia, are significant dif-

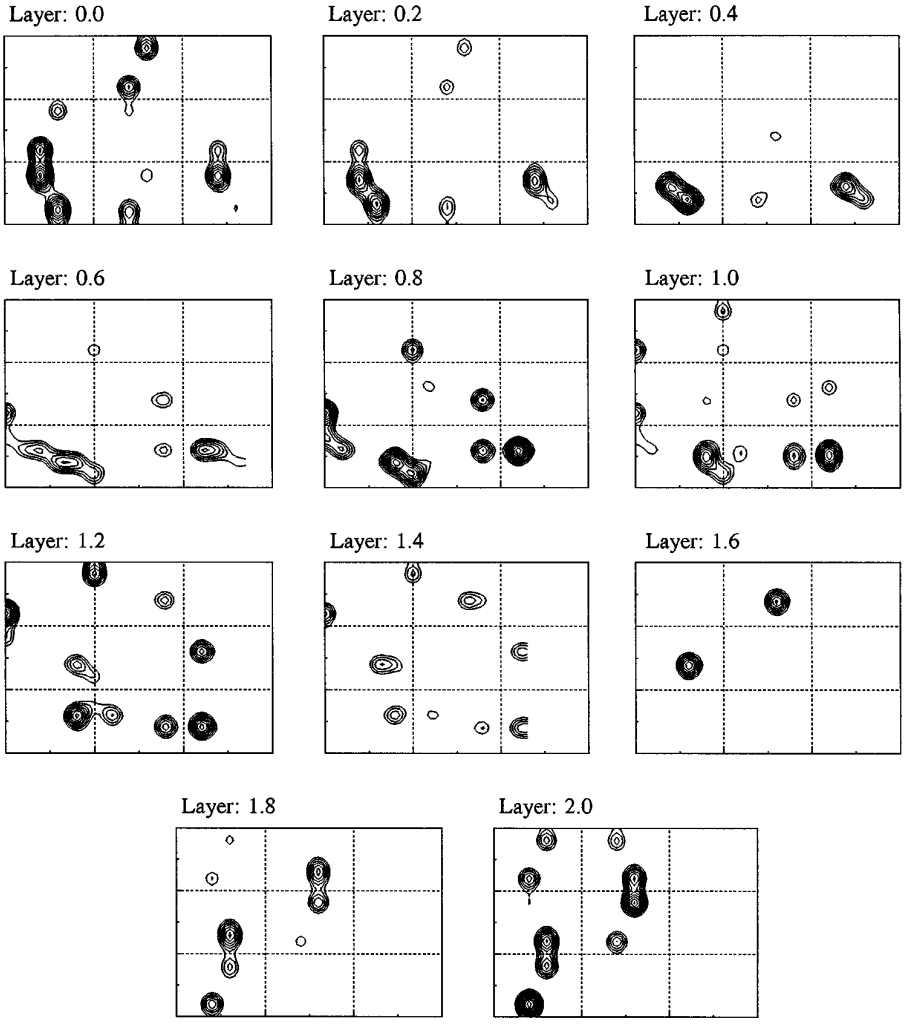

FIG. 3. Intensities of the diffuse scattering of zirconia calculated by superposition of all symmetrically diffuse maxima. For details see the text. Each frame shows the identical section in reciprocal space as its corresponding frame in Fig. 2.

fuse features. The observed additional diffuse scattering between the layers of the $[1\bar{1}0]$ zone can be explained by intersections with diffuse maxima of symmetrically equivalent $[1\bar{1}0]$ zones as shown by the simple calculations presented in this paper. This observation agrees with our previous quantitative analysis of the diffuse scattering of calcium-stabilized zirconia. We have, however, no evidence for more extended diffuse scattering as reported for yttrium-stabilized zirconia (6). A comparison of the $\frac{1}{2}c^*$ plane, i.e., $(hkl)[001] = 0.5$, extracted from our measurements with the observations in (6) and notably (7) shows a qualitative agreement of the diffuse scattering of zirconia doped with CaO and Y_2O_3. Our observed diffuse maxima are very similar to the diffuse maxima of CSZ with 12 mol% Ca (7, Fig. 2d). As for the different layers of the $[1\bar{1}0]$ zone, the diffuse maxima in the $\frac{1}{2}c^*$ plane can be described as the intersection of diffuse maxima of symmetrically equivalent [110] zones as seen in Fig. 4. Inspection of Fig. 4 shows that the halfwidth of the diffuse maxima is also about 0.25 reciprocal lattice units in the $[\bar{1}10]$ direction, i.e., perpendicular to the measured layers extracted from our 3D measurements. Electron diffraction patterns of 19 mol% CaO (10 Fig. 2b) and 50% $TbO_{1.5}$ (7 Fig. 2e), both taken down the $[11\bar{2}]$ zone, show maxima slightly shifted along $[1\bar{1}0]$ from the $\frac{1}{2}\{111\}$ and $\frac{1}{2}\{333\}$ reciprocal positions. The second of these pairs of maxima coincides with the maximum in the lower left section of the layer 0.4 in our measurement at reciprocal vector 1.7 1.3 1.5, Fig. 2. In addition, the electron diffraction patterns show complete rings of diffuse scattering around $\frac{1}{2}\{3\bar{1}1\}$ and $\frac{1}{2}\{513\}$. These rings are not observed by X-ray diffraction. At reciprocal vector 2.5 0.5 1.5 (lower left section of layer 2.0 in Fig. 2) diffuse maxima appear that do not form a ring normal to $[11\bar{2}]$. The formation of a complete ring in

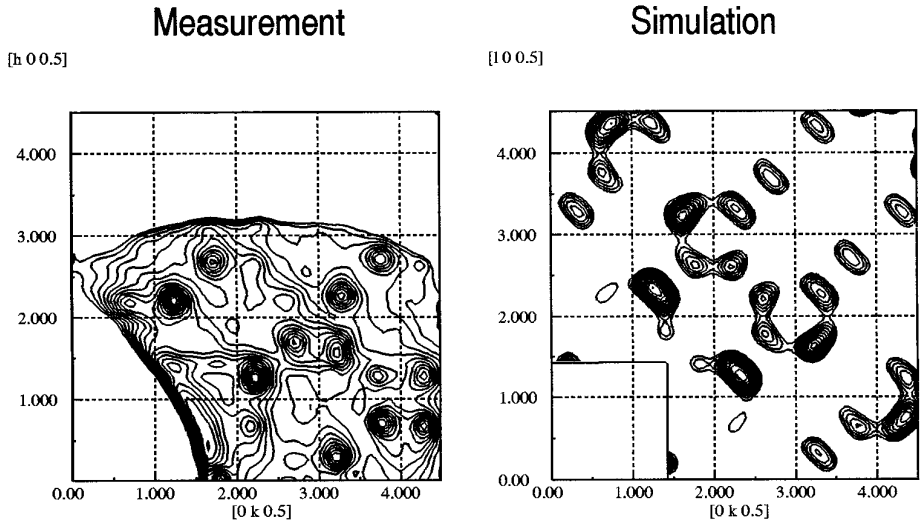

FIG. 4. Extracted and simulated plane $\frac{1}{2}c^*$ of zirconia. The intensities are given in steps of 50 counts; the lowest intensity level corresponds to 5 counts.

the electron diffraction pattern, however, is due to multiple scattering and cannot be expected to be observed by X-ray diffraction (12). Subsequently the X-ray diffraction patterns normal to [111] (7, Fig. 2c) do not show complete rings but rather arcs of diffuse scattering. Similar arcs normal to [111] are found in our measurements only around $\frac{1}{2}\{333\}$ (Fig. 2). The diffuse maxima at 1.4 1.4 1.8, 1.6 1.6 1.2, and 1.8 1.4 1.4 in layers 0.0, 0.2, and 0.4, respectively, overlap causing an arc-shaped diffuse scattering. The calculated maxima in Fig. 3 reproduce this feature quite well. We feel that this work strongly supports our previous observation that the main diffuse features in zirconia are diffuse maxima located in the layers of the $[1\bar{1}0]$ zones and can be indexed by satellite vectors of $\pm(0.4\ 0.4\ \pm 0.8)$.

ACKNOWLEDGMENT

This work was supported by funds of the BMFT under 05 5WMIAB 7.

REFERENCES

1. E. C. Subbaro, *in* "Advances in Ceramics" (A. H. Heuer and L. W. Hobbs, Eds.), Vol. 3, p. 1. 1981.
2. S. M. Ho, *Mater. Sci. Eng.* **54,** 23 (1982).
3. R. B. Neder, F. Frey, and H. Schulz, *Acta. Crystallogr. Sect. A* **46,** 799 (1990).
4. Th. Proffen, R. B. Neder, F. Frey, and W. Assmus, *Acta. Crystallogr. Sect. B* **49,** 599 (1993).
5. Th. Proffen, R. B. Neder, and F. Frey, *Acta. Crystallogr. Sect. B* **52,** 59 (1996).
6. T. R. Welberry, R. L. Withers, J. G. Thompson, and B. D. Bultler, *J. Solid State Chem.* **100,** 71 (1992).
7. T. R. Welberry, R. L. Withers, and S. C. Mayo, *J. Solid State Chem.* **115,** 43 (1995).
8. R. B. Neder, *J. Appl. Crystallogr.* **27,** 845 (1994).
9. R. B. Neder, Th. Proffen, M. Burghammer, F. Frey, and H. Schulz, in preparation.
10. R. Miida, M. Tanaka, H. Arashi, and M. Ishigame, *J. Appl. Crystallogr.* **27,** 67 (1994).
11. Th. Proffen, Dissertation, University Munich, 1995.
12. R. L. Withers, personal communication, 1996.